

Triplet state CPL active helicene-dithiolene platinum bipyridine complexes

Thomas Biet, Thomas Cauchy, Qinchao Sun, Jie Ding, Andreas Hauser,* Patric Oulevey,
Thomas Bürgi, Denis Jacquemin, Nicolas Vanthuyne, Jeanne Crassous and Narcis Avarvari*

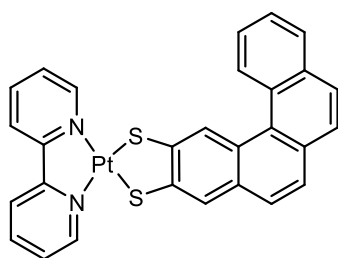
SUPPORTING INFORMATION

Experimental section

General comments. Dry THF and ether were obtained from a solvent purification system (LC Technology Solutions Incorporated). Nuclear magnetic resonance spectra were recorded on a Bruker Advance DRX 300 spectrometer operating at 300 MHz for ^1H and 75 MHz for ^{13}C . Chemical shifts are expressed in parts per million (ppm) downfield from external TMS. The following abbreviations are used: s, singlet; d, doublet; t, triplet; m, multiplet. MALDI-TOF MS spectra were recorded on a Bruker Biflex-IIITM apparatus, equipped with a 337nm N_2 laser. Elemental analyses were recorded using Flash 2000 Fisher Scientific Thermo Electron analyzer. IR spectra were recorded on Bruker FT-IR Vertex 70 spectrometer equipped with a Platinum diamond ATR accessory. The precursors **1a,b** were prepared according to the literature procedure.^[1] (*M*) and (*P*) enantiomers of **1b** were separated by chiral HPLC from a solution of (*rac*)-**1b**.

(bpy)Pt([4]helicene-dithiolene)

2a



3,3'-(benzo[*c*]phenanthrene-2,3-diylbis(sulfaneydiyl))dipropanenitrile **1a** (150 mg, 0.38 mmol) and caesium hydroxide hydrate (130 mg, 0.77 mmol), were placed in a Schlenk and dissolved in DMF/MeOH (15 mL) solvent mixture. The resulting solution was stirred for 1.5 h, while the colour changed to yellow. Pt(bipy)Cl₂^[2] (160 mg, 0.38 mmol) was then added to the solution, and the reaction mixture, which became dark purple, was stirred overnight. After partial evaporation of solvent in vacuo diethyl ether (20 mL) was added to the remaining solution to precipitate the complex. The precipitate was filtered and washed with diethyl ether. After a flash chromatography over SiO₂ (CH₂Cl₂ as eluent), **2a** was obtained as a dark purple solid (241 mg, 82%). Suitable single crystals for X-ray analysis have been grown by slow diffusion of cyclohexane into a CH₂Cl₂ solution of **2a**.

-
- (1) Biet, T.; Fihey, A.; Cauchy, T.; Vanthuynne, N.; Roussel, C.; Cras-sous, J.; Avarvari, N. *Chem. Eur. J.* **2013**, *19*, 13160–13167.
 - (2) Newkome, G. R.; Theriot, K. J.; Fronczek, F. R.; Villa, B. *Organometallics* **1989**, *8*, 2513–2523.

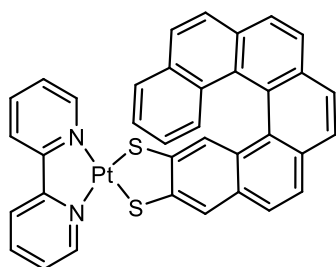
$^1\text{H NMR}$ (DMSO, 300 MHz) δ (ppm): 9.20 (d, $J = 5.6$ Hz, 1H), 9.14 (d, $J = 5.7$ Hz, 1H), 9.10 (d, $J = 8.4$ Hz, 1H), 8.96 (s, 1H), 8.74 (d, $J = 8.1$ Hz, 2H), 8.43 (t, $J = 8.6$ Hz, 2H), 8.13 (d, $J = 8.3$ Hz, 1H), 7.98-7.75 (m, 7H), 7.74-7.65 (m, 2H).

MS (MALDI-TOF) $m/z = 641.1$ (M^+).

Elemental analysis calcd. (%) for $\text{C}_{28}\text{H}_{18}\text{N}_2\text{PtS}_2$: C 52.41, H 2.83, N 4.37, S 9.99; found: C 52.22, H 2.95, N 4.21, S 10.18.

(bpy)Pt([6]helicene-dithiolene)

(rac)-2b



3,3'-(hexahelicene-10,11-diylbis(sulfanediy))dipropanenitrile (*rac*)-**1b** (100 mg, 0.20 mmol) and caesium hydroxide hydrate (70 mg, 0.42 mmol), were placed in a Schlenk and dissolved in DMF/MeOH (10 mL) solvent mixture. The resulting solution was stirred for 1.5 h, while the colour changed to yellow. Pt(bipy)Cl₂ (85 mg, 0.20 mmol) was then added to the solution, and the resulting reaction mixture, from which a precipitate started to appear, was stirred overnight. Diethyl ether (20 mL) was added to the reaction mixture and the precipitate was filtered and washed with diethyl ether. After a flash chromatography over SiO₂ (CH₂Cl₂ as eluent) (*rac*)-**2b** was obtained as a dark purple solid (106 mg, 71%). Suitable single crystals for X-ray analysis have been grown by slow diffusion of cyclohexane into a benzonitrile solution of (*rac*)-**2b**.

$^1\text{H NMR}$ (DMSO, 300 MHz) δ (ppm): 9.51 (d, $J = 5.7$ Hz, 1H), 9.03 (d, $J = 5.2$ Hz, 1H), 8.80 (d, $J = 5.8$ Hz, 1H), 8.74-8.56 (m, 2H), 8.52-8.31 (m, 2H), 8.29-7.68 (m, 10H), 7.66 (d, $J = 8.3$ Hz, 1H), 7.59 (d, $J = 8.2$ Hz, 1H), 7.43 (s, 1H), 7.28 (t, $J = 7.6$ Hz, 1H), 6.79 (t, $J = 7.4$ Hz, 1H).

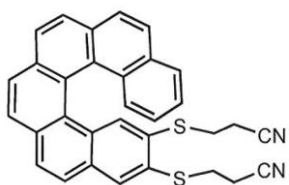
MS (MALDI-TOF) $m/z = 741.1$ (M^+).

Elemental analysis calcd. (%) for $\text{C}_{36}\text{H}_{22}\text{N}_2\text{PtS}_2$: C 58.29, H 2.99, N 3.78, S 8.64; found: C 58.13, H 2.95, N 3.94, S 8.87.

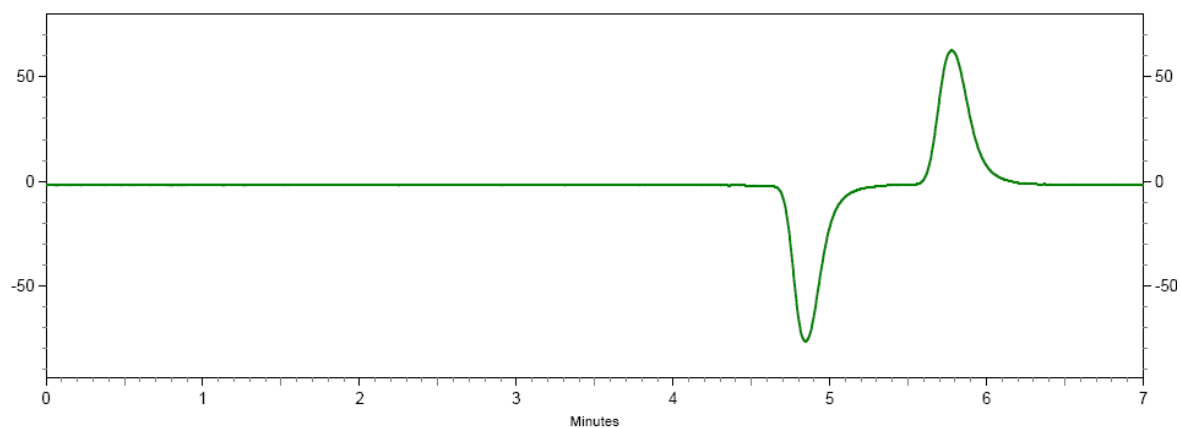
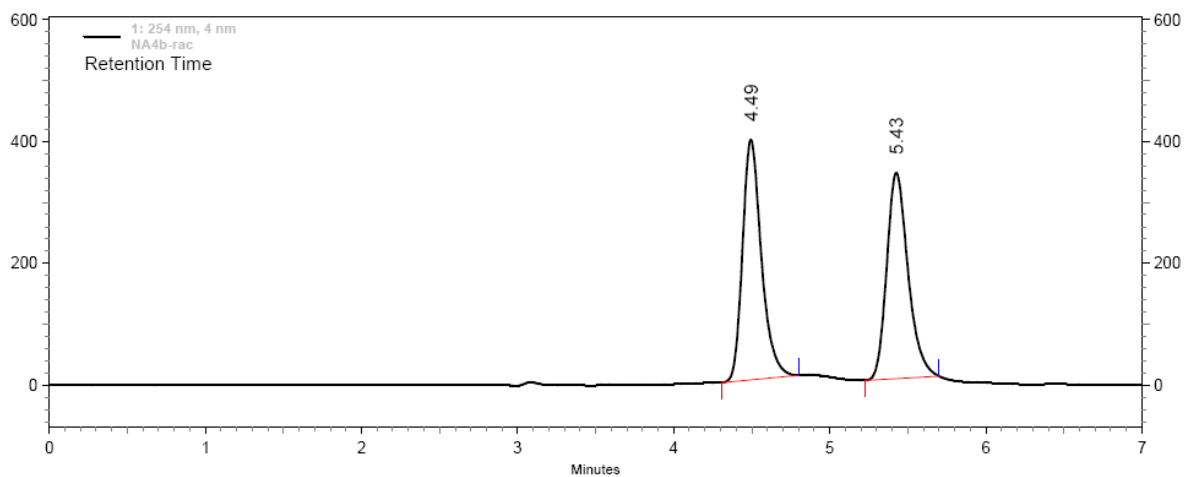
Enantiopure (*M*)-**2b** and (*P*)-**2b** have been prepared similarly as (*rac*)-**2b** starting from (*M*)-**1b** and (*P*)-**1b**, respectively.

Chiral HPLC

Analytical chiral HPLC separation for compound **1b**



The sample is dissolved in chloroform, injected on the chiral column, and detected with an UV and CD detectors at 254 nm. The flow-rate is 1 ml/min.



1: 254 nm, 4 nm

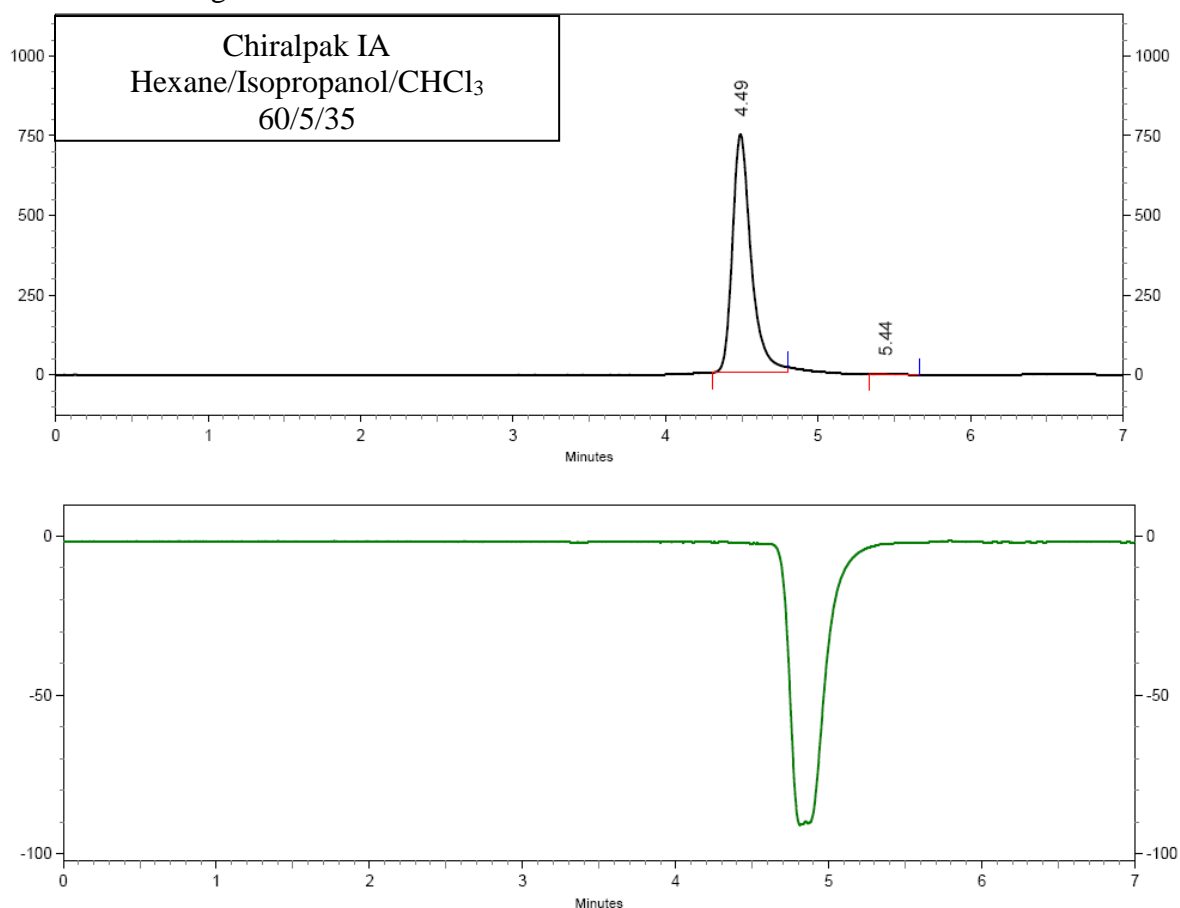
Results

| Retention Time | Area | Area % | Capacity factor | Relative RT | Resolution (US) |
|----------------|----------|--------|-----------------|-------------|-----------------|
| 4.49 | 13260708 | 50.84 | 0.50 | 1.00 | 0.00 |
| 5.43 | 12822627 | 49.16 | 0.81 | 1.63 | 4.01 |

Fig. S1 Analytical chiral HPLC separation for compound **1b**

Semi-preparative separation for compound **1b** :

- Sample preparation: About 46 mg of compound **1b** are dissolved in 6 mL of chloroform.
- Chromatographic conditions: Chiralpak IA (250 x 10 mm), thermostated at 25°C, Hexane/Isopropanol/CHCl₃ 60/5/35 as mobile phase, flow-rate = 5 mL/min, UV detection at 254 nm.
- Injections (stacked injections): 60 times 100 µL, every 3 minutes.
- Collection: the first eluted enantiomer is collected between 0.2 and 1.2 minutes and the second one between 2.0 and 3.5 minutes.
- First fraction: 22 mg of the first eluted ((-)_{CD254}-enantiomer, $\alpha_D^{25} = + 2900$ (c = 0.023, CHCl₃)) with an enantiomeric excess higher than 99.5 %.
- Second fraction: 22 mg of the second eluted ((+)_{CD254}-enantiomer $\alpha_D^{25} = - 2900$ (c = 0.023, CHCl₃)) with an enantiomeric excess higher than 99 %.
- Chromatograms of the collected enantiomers:



1: 254 nm, 4 nm

Results

| Retention Time | Area | Area % | Capacity factor | Relative RT | Resolution (USP) |
|----------------|----------|--------|-----------------|-------------|------------------|
| 4.49 | 25567668 | 99.83 | 0.50 | 1.00 | 0.00 |
| 5.44 | 42927 | 0.17 | 0.81 | 0.00 | 4.22 |

Fig. S2 Chiral HPLC separation for compound (*P*)-**1b**

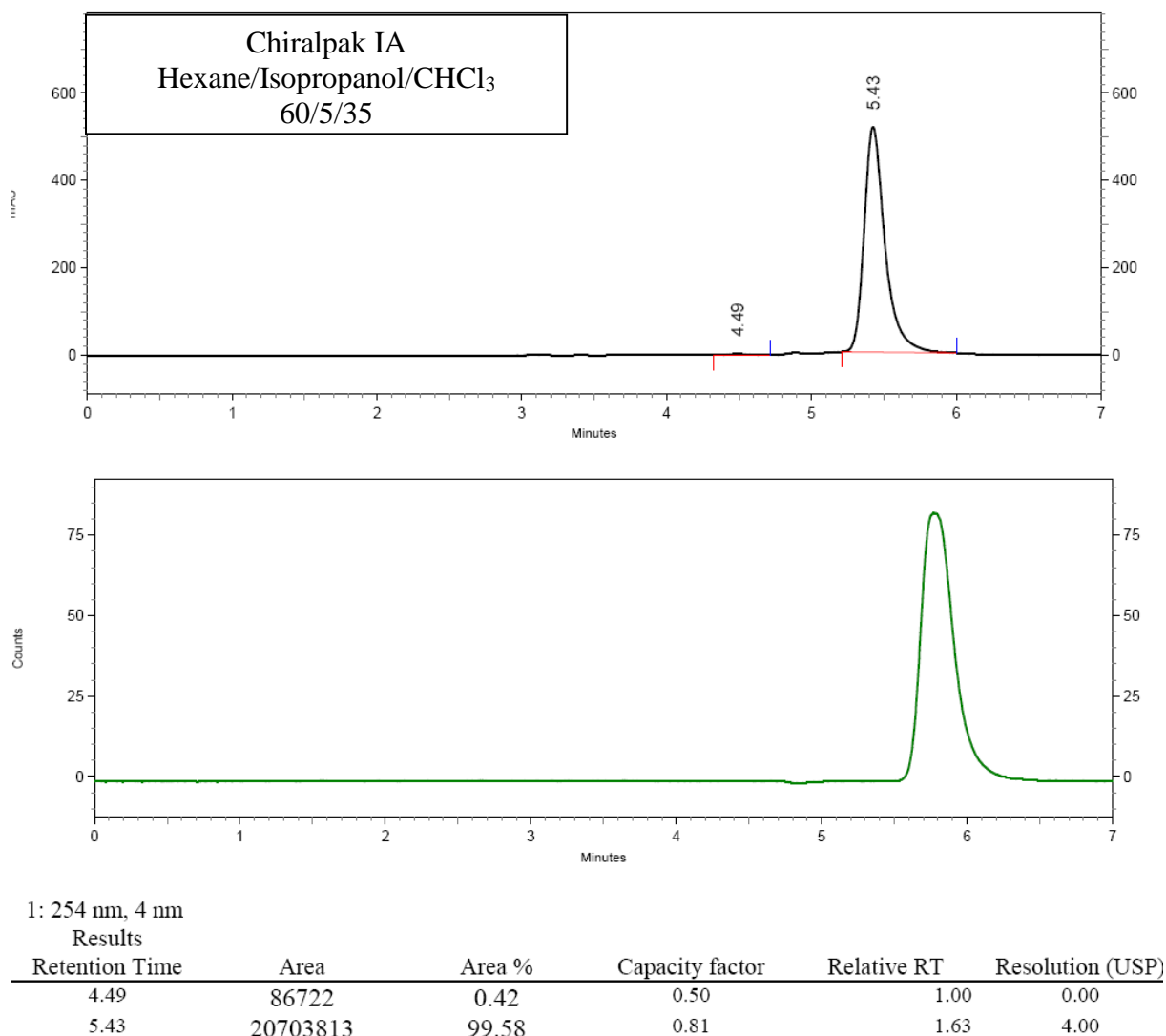


Fig. S3 Chiral HPLC separation for compound (*M*)-**1b**

X-Ray structure determinations

Details about data collection and solution refinement are given in Tables S1 and S2. X-ray diffraction measurements were performed on a Bruker Kappa CCD diffractometer, operating with a $\text{MoK}\alpha$ ($\lambda=0.71073 \text{ \AA}$) X-ray tube with a graphite monochromator, for (*rac*)-**2a** and (*rac*)-**2b**, while for (*M*)-**2b** X-ray single-crystal diffraction data were collected at 150 K on an Agilent SuperNova diffractometer equipped with Atlas CCD detector and mirror monochromated micro-focus $\text{Cu-K}\alpha$ radiation ($\lambda = 1.54184 \text{ \AA}$).

The structures (*rac*)-**2a** and (*rac*)-**2b** were solved (SHELXS-97) by direct methods and refined (SHELXL-97) by full matrix least-square procedures on F^2 . All non-H atoms were

refined anisotropically. Hydrogen atoms were introduced at calculated positions (riding model), included in structure factor calculations but not refined. The structure (*M*)-**2b** was solved by direct methods, expanded and refined on F^2 by full matrix least-squares techniques using SHELXS97 (G.M. Sheldrick, 1998) and SHEXL-2013 (G. M. Sheldrick 1993-2013, Version 2013/4) programs. All non-H atoms were refined anisotropically and multiscan empirical absorption was corrected using CrysAlisPro program (CrysAlisPro, Agilent Technologies, V1.171.37.35g, 2014). The H atoms were included in the calculation without refinement.

Crystallographic data for the four structures have been deposited with the Cambridge Crystallographic Data Centre, deposition numbers CCDC 1550054 (*(rac)*-**2a**), 1550055 (*(rac)*-**2b**), 1550056 (*(M)*-**2b**). These data can be obtained free of charge from CCDC, 12 Union road, Cambridge CB2 1EZ, UK (e-mail: deposit@ccdc.cam.ac.uk or <http://www.ccdc.cam.ac.uk>).

Table S1. Crystal Data and Structure Refinement for *(rac)*-**2a**, *(rac)*-**2b** and *(M)*-**2b**.

| Compound | <i>(rac)</i> - 2a | <i>(rac)</i> - 2b | <i>(M)</i> - 2b |
|---|---|---|---|
| empirical formula | C ₂₉ H ₂₀ Cl ₂ N ₂ PtS ₂ | C ₃₆ H ₂₂ Cl ₂ N ₂ PtS ₂ | C ₁₆₈ H ₁₃₆ N ₈ Pt ₄ S ₈ |
| fw | 546.72 | 741.77 | 3303.69 |
| <i>T</i> (K) | 293(2) | 293(2) | 150.0(1) |
| wavelength (Å) | 0.71073 | 0.71073 | 1.54184 |
| cryst syst | Monoclinic | Triclinic | Orthorhombic |
| space group | <i>C</i> 2/ <i>c</i> | <i>P</i> -1 | <i>P</i> 2 ₁ 2 ₁ 2 ₁ |
| <i>a</i> (Å) | 20.358 (7) | 9.7082 (5) | 21.1835 (3) |
| <i>b</i> (Å) | 7.9519 (14) | 10.5020 (6) | 21.2582 (3) |
| <i>c</i> (Å) | 33.160 (3) | 13.5980 (9) | 27.7753 (4) |
| α (deg) | 90.00 | 85.164 (5) | 90.00 |
| β (deg) | 107.080 (7) | 77.659 (5) | 90.00 |
| γ (deg) | 90.00 | 88.955 (4) | 90.00 |
| <i>V</i> (Å ³) | 5131.3 (10) | 1349.53 (14) | 12507.9 (3) |
| <i>Z</i> | 8 | 2 | 4 |
| <i>D_c</i> (g cm ⁻³) | 1.881 | 1.825 | 1.754 |
| abs coeff (mm ⁻¹) | 5.863 | 5.384 | 9.912 |
| cryst size (mm ³) | 0.6 × 0.4 × 0.2 | 0.3 × 0.1 × 0.05 | 0.23 × 0.03 × 0.03 |
| Flack parameter | | | -0.009 (7) |
| GOF on F^2 | 1.215 | 1.077 | |
| final <i>R</i> indices [$I > 2\sigma(I)$] | R1 = 0.0336, wR2 = 0.0733 | R1 = 0.0461, wR2 = 0.0699 | R1 = 0.0386, wR2 = 0.0924 |
| <i>R</i> indices (all data) | R1 = 0.0483, wR2 = 0.0793 | R1 = 0.0871, wR2 = 0.0818 | R1 = 0.0481, wR2 = 0.1017 |

$$^a R(F_o) = \frac{\sum ||F_o| - |F_c||}{\sum |F_o|}; R_w(F_o^2) = \left[\frac{\sum [w(F_o^2 - F_c^2)^2]}{\sum [w(F_o^2)^2]} \right]^{1/2}$$

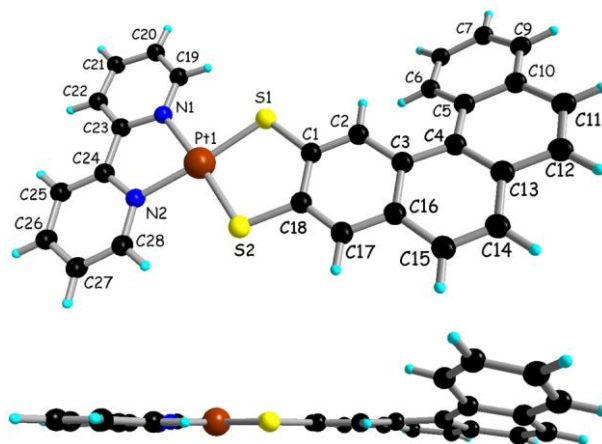
Complex (*rac*)-2a

Fig. S4 Molecular structure of (*rac*)-2a together with the atom numbering scheme (top) and a side view (bottom).

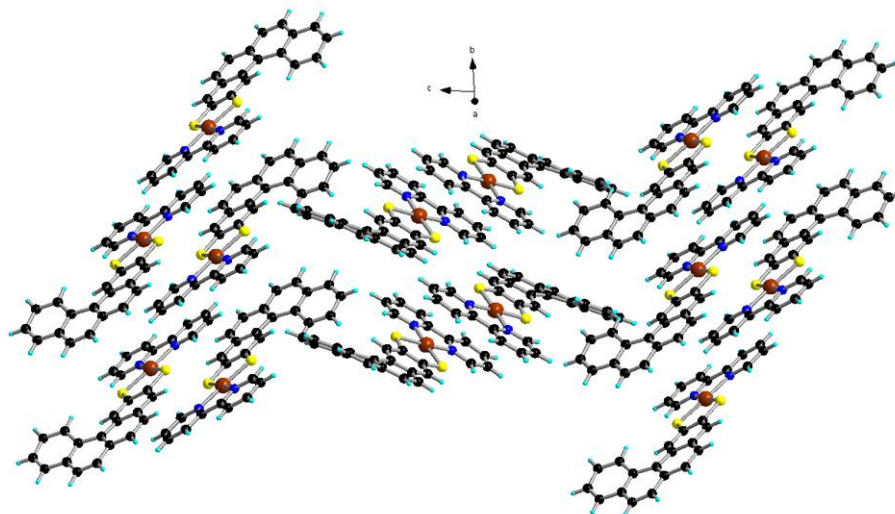


Fig. S5 Packing diagram for (*rac*)-2a.

Table S2. Selected lengths (Å) and angles (°) for (*rac*)-2a•CH₂Cl₂

| Distances (Å) | | Dihedral Angle between two planes(°) (calc) |
|---------------|------------|---|
| Pt(1)-N(1) | 2.056(4) | C(1)-C(2)-C(3)-C(16)-C(17)-C(18) & C(5)-C(6)-C(7)-C(8)-C(9)-C(10) |
| Pt(1)-N(2) | 2.052(4) | |
| Pt(1)-S(1) | 2.2525(12) | 25.40 |
| Pt(1)-S(2) | 2.2642(13) | |
| S(1)-C(1) | 1.752(5) | |
| S(2)-C(18) | 1.758(5) | |
| N(1)-C(19) | 1.335(6) | |
| N(1)-C(23) | 1.354(6) | |
| N(2)-C(28) | 1.339(6) | |
| N(2)-C(24) | 1.340(6) | |

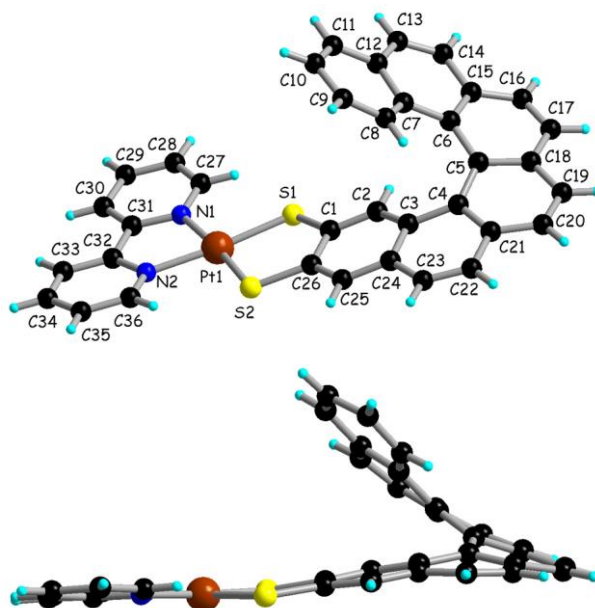
Complex (*rac*)-**2b**

Fig. S6 Molecular structure of (*rac*)-**2b** together with the atom numbering scheme (top) and a side view (bottom).

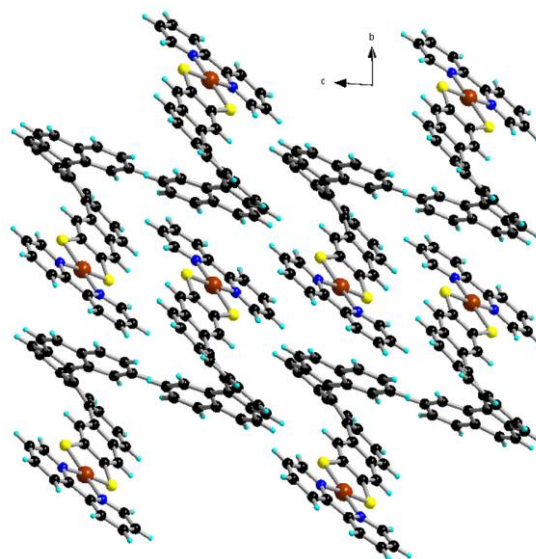


Fig. S7 Packing diagram for (*rac*)-**2b**.

Table S3. Selected lengths (Å) and angles (°) for (*rac*)-**2b**

| Distances (Å) | | Dihedral Angle between two planes (°) (calc) |
|---------------|------------|--|
| Pt(1)-N(1) | 2.061(6) | C(1)-C(2)-C(3)-C(24)-C(25)-C(26) & C(7)-C(8)-C(9)-C(10)-C(11)-C(12) 53.76 |
| Pt(1)-N(2) | 2.050(5) | |
| Pt(1)-S(1) | 2.2579(18) | |
| Pt(1)-S(2) | 2.2527(19) | |
| S(1)-C(1) | 1.751(7) | |
| S(2)-C(26) | 1.745(7) | |
| N(1)-C(27) | 1.326(9) | |
| N(1)-C(31) | 1.359(9) | |
| N(2)-C(32) | 1.367(9) | |
| N(2)-C(36) | 1.341(9) | |

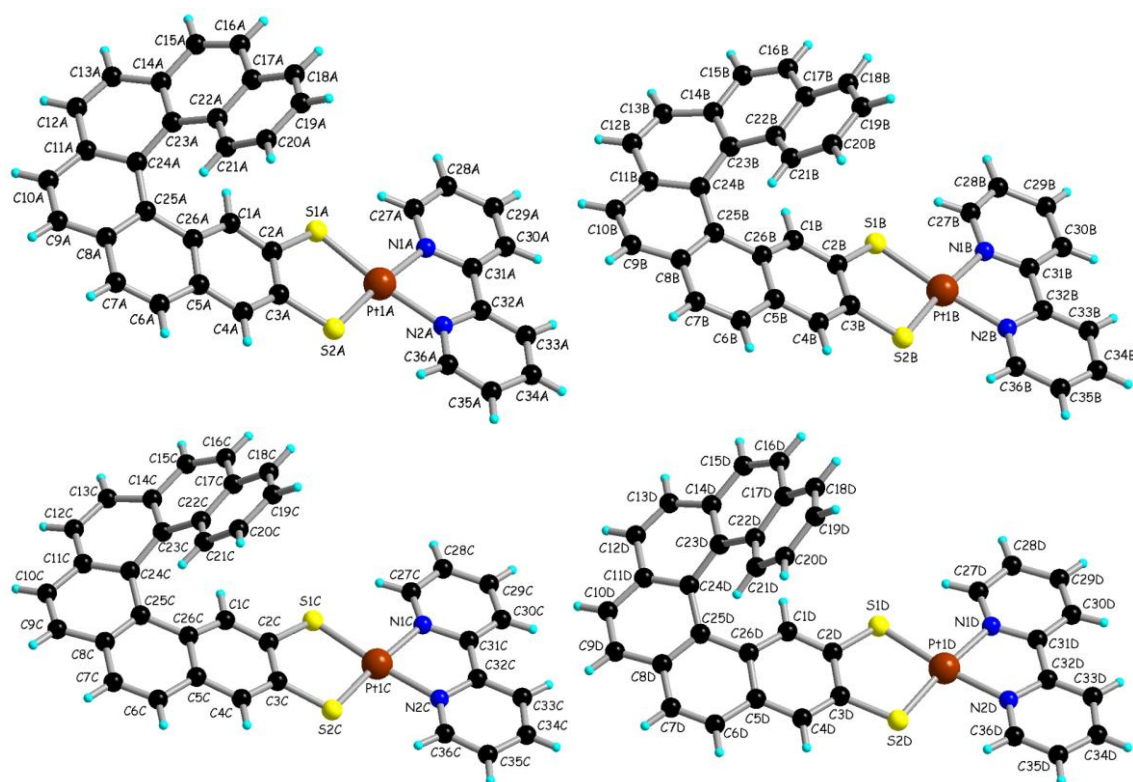
Complex (*M*)-2b

Fig. S8 Molecular structure of (*M*)-2b with a view of the four independent molecules Pt1A, Pt1B, Pt1C and Pt1D.

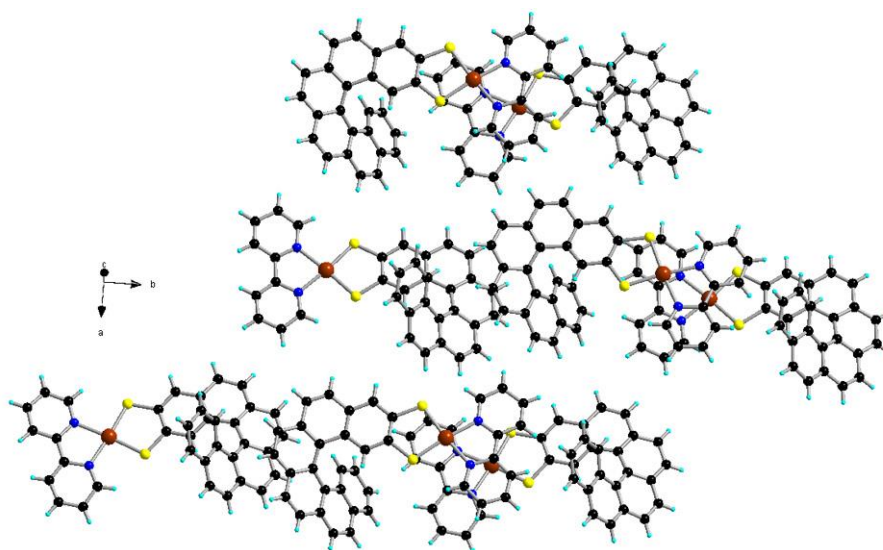


Fig. S9 Packing diagram for (*M*)-2b.

Table S4. Selected lengths (Å) and angles (°) for (*M*)-2b for the four independent molecules

| Distances (Å) | | Dihedral Angle between two planes(°) (calc) |
|---------------|------------|--|
| Pt1A-N1A | 2.054(7) | C1A-C2A-C3A-C4A-C5A-C26A & C17A-C18A-C19A-C20A-C21A-C22A |
| Pt1A-N2A | 2.065(6) | |
| Pt1A-S1A | 2.2471(18) | |
| | | 58.71 |

| | | |
|---------------|-----------|---|
| Pt1A-S2A | 2.249(2) | |
| S1A-C2A | 1.772(8) | |
| S2A-C3A | 1.768(9) | |
| Distances (Å) | | Dihedral Angle between two planes(°) (calc) |
| Pt1B-N1B | 2.068(9) | C1B-C2B-C3B-C4B-C5B-C26B & C17B-C18B-C19B-C20B-C21B-C22B 60.53 |
| Pt1B-N2B | 2.065(7) | |
| Pt1B-S1B | 2.258(2) | |
| Pt1B-S2B | 2.248(3) | |
| S1B-C2B | 1.747(10) | |
| S2B-C3B | 1.753(9) | |
| Distances (Å) | | Dihedral Angle between two planes(°) (calc) |
| Pt1C-N1C | 2.071(8) | C1C-C2C-C3C-C4C-C5C-C26C & C17C-C18C-C19C-C20C-C21C-C22C 58.58 |
| Pt1C-N2C | 2.072(7) | |
| Pt1C-S1C | 2.255(2) | |
| Pt1C-S2C | 2.252(2) | |
| S1C-C2C | 1.758(9) | |
| S2C-C3C | 1.759(7) | |
| Distances (Å) | | Dihedral Angle between two planes(°) (calc) |
| Pt1D-N1D | 2.072(7) | C1D-C2D-C3D-C4D-C5D-C26D & C17D-C18D-C19D-C20D-C21D-C22D 62.36 |
| Pt1D-N2D | 2.062(8) | |
| Pt1D-S1D | 2.257(2) | |
| Pt1D-S2D | 2.254(2) | |
| S1D-C2D | 1.749(8) | |
| S2D-C3D | 1.759(9) | |

Photophysical studies

UV-Vis absorption spectra were recorded on a Cary 5000 spectrophotometer. Steady-state emission spectra were recorded on a Fluorolog 3 spectrophotometer. Luminescence quantum yields were calculated relative to the quantum yield of $[\text{Ru}(\text{bpy})_3]^{2+}$ by comparing the luminescence intensities for irradiation at a wavelength of equal absorption. According to Crosby et al. (J. Phys. Chem., 1971, 75, 991), the luminescence quantum yield of $[\text{Ru}(\text{bpy})_3]^{2+}$ at room temperature in acetonitrile is ca. 0.062.

CH_3CN extra dry from ACROS, and CH_2Cl_2 analytical from Fluka, were used as received without further purification. For the preparation of (*rac*)-**2a** solution, a stock solution in dichloromethane (DCM) with concentration about 10^{-4} M was prepared, and all other solutions were diluted from the stock solution (the volume proportion of DCM was less than 5 % in all of the tested solution samples). However, a solution with concentration about 10^{-4} M was directly prepared for (*rac*)-**2b**.

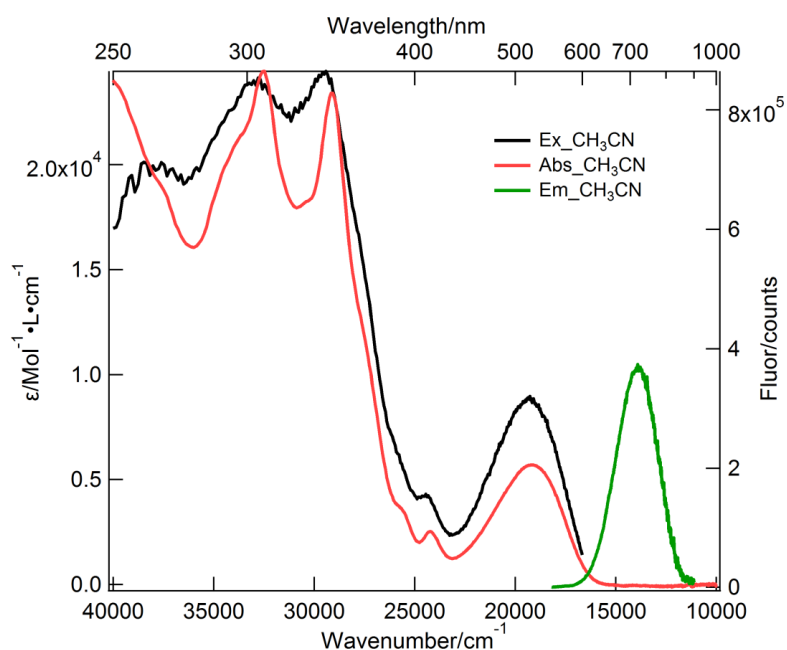


Fig. S10 Absorption, emission and excitation spectra of (*rac*)-**2a** in CH_3CN . The absorption spectrum was measured for a concentration of 2.2×10^{-5} M. Emission was measured for excitation at 525 nm in CH_3CN and a concentration of 2.2×10^{-5} M, degassed by nitrogen for 20 min. Excitation was measured at an emission wavelength of 720 nm.

Table S5. Absorption and Emission properties of (*rac*)-**2a** and (*rac*)-**2b**, measured at room temperature

| Sample | Absorption (MLCT) ^a /nm | ϵ (MLCT) ^a /mol ⁻¹ Lcm ⁻¹ | Emission ^a /nm | Quantum yield ^c (%) |
|---------------------------|------------------------------------|--|---------------------------|--------------------------------|
| (<i>rac</i>)- 2a | 550 | 6713 | 720 | 0.186 ^b |
| (<i>rac</i>)- 2b | 562 | 3637 | 715 | 0.147 ^a |

^a measurements performed in CH₂Cl₂, and ^b in CH₃CN

^c [Ru(bpy)₃]²⁺ in CH₃CN as a reference luminescence compound

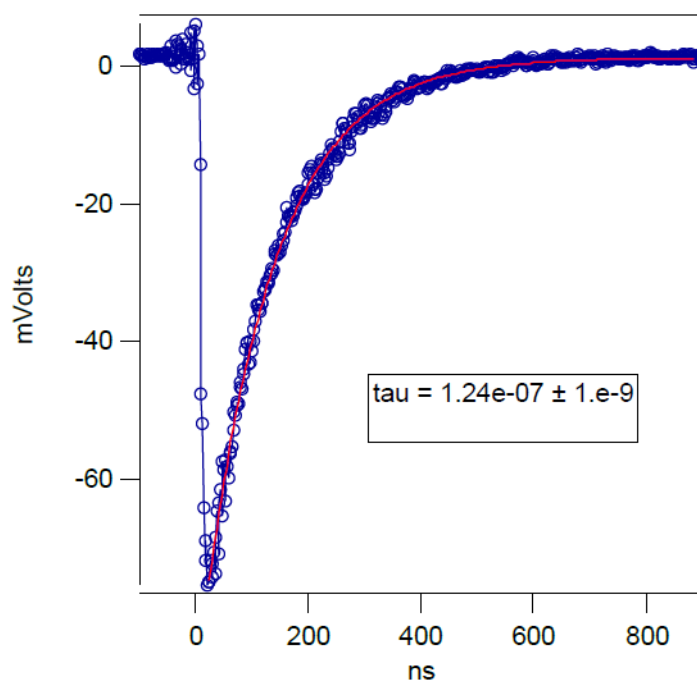


Fig. S11 Luminescence decay curve of (*M*)-**2b** measured at 735 nm in deoxygenated acetonitrile at room temperature and excitation at 458 nm.

TD-DFT calculations

To rationalize the UV-visible absorption and emission properties of these coordination compounds, we relied on Time Dependent Density Functional Theory (TD-DFT) method which has been shown to generally an excellent tool to assess CPL properties.^[2-4] We have selected as workhorse the hybrid M06 functional known to be effective for metal complexes.^[5] This functional, that contains 27% of *exact* exchange is rather similar to the PBE0 hybrid,^[6-7] that contains 25% of *exact* exchange and was used successfully employed in a previous helicenes study.^[8] To ascertain that our results are not strongly dependent on the selected functional, several supplementary calculations have been performed with Truhlar's M06-2X that encompasses 54% of *exact* exchange.^[5] Our calculations consisted in geometry optimizations performed starting from the X-ray structures, subsequent frequency calculations and TD-DFT calculations of the excited-state. For a compound with a large aromatic moiety and a heavy metal atom, a large basis set with polarization functions is mandatory, and the addition of diffuse functions is also necessary during the simulation of electronic transitions. Therefore, during the geometry optimizations, we selected the 6-311G(d,p) atomic basis for all atoms but for the platinum center that was described with the LanL2TZ(f) basis set and pseudo-potentials, whereas, during the TD-DFT calculations, the 6-311+G(2d,p) atomic basis set was used for all non-metallic atoms [LanL2TZ(f) for Pt]. For the absorption properties the first forty singlet electronic excited-states were calculated for both the [4]helicene and [6]helicene compounds. As the photophysical studies indicate that emission is originating from phosphorescence, we also optimized the lowest T1 state, at the same level of theory as the ground-state using unrestricted DFT. This allowed giving access to an estimate of the emission energies with DFT. Our calculations have systematically considered solvent effects as described by the well-known PCM model (acetonitrile), using the linear-response approach in its non-equilibrium limit for the TD-DFT calculations. All calculations were made by the Gaussian09 program,^[9] whereas the data exploitation was in part generated by an homemade program using CCLIB parser.^[10-11] To estimate the CT characteristics, we relied on the d_{CT} metric of Le Bahers.^[12]

Geometry optimization

Below is a comparison between the X-Ray and computed (PCM-DFT) data for selected geometrical parameters. Given the fact that the two are obtained in a different medium, the agreement is certainly satisfactory.

Table S6. Experimental (from X-ray diffraction) and theoretical geometric parameters

| | <i>(rac)</i> - 2a EXP | <i>(M)</i> - 2a CALC | <i>(rac)</i> - 2b EXP | <i>(P)</i> - 2b CALC |
|----------------------------------|------------------------------|-----------------------------|------------------------------|-----------------------------|
| Pt-S distances (Å) | 2.252 / 2.264 | 2.311 / 2.312 | 2.253 / 2.256 | 2.312 / 2.310 |
| Pt-N distances (Å) | 2.056 / 2.0252 | 2.088 / 2.088 | 2.050 / 2.061 | 2.088 / 2.089 |
| Cycles 1-4/6 dihedral angles (°) | 28.4 | 28.1 | 58.7 | 41.7 |

(M)-**2a**

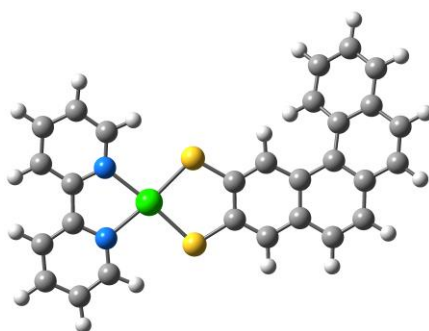


Fig. S12 Equilibrium geometry for *(M)*-**2a** obtained at the M06 level.

Equilibrium ground-state geometry and energy [M06 level]

Total electronic energy -2102.35623266 au

Cartesian coordinates (in Å)

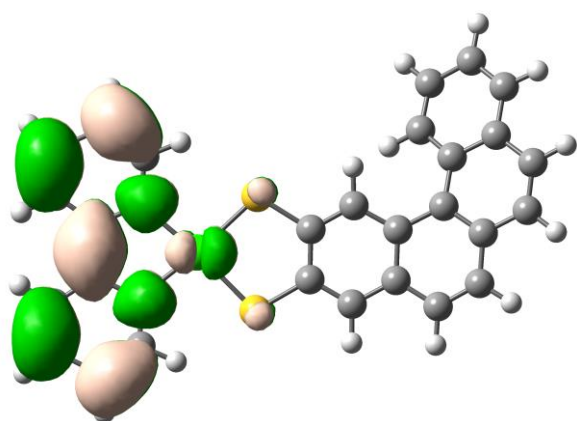
| | | | |
|----|------------|------------|------------|
| C | 4.2315450 | -2.2634310 | 0.2725510 |
| N | 3.9721420 | -0.9592020 | 0.1148300 |
| C | 5.0022980 | -0.0853340 | 0.0198930 |
| C | 6.3175060 | -0.5248490 | 0.0863280 |
| C | 6.5803090 | -1.8721270 | 0.2509610 |
| C | 5.5181030 | -2.7576940 | 0.3453050 |
| Pt | 2.0693170 | -0.1072230 | 0.0019280 |
| N | 3.2961880 | 1.5690650 | -0.2050630 |
| C | 2.8701810 | 2.8282430 | -0.3667630 |
| C | 3.7397330 | 3.8935680 | -0.4842340 |
| C | 5.1036010 | 3.6513870 | -0.4335770 |
| C | 5.5482460 | 2.3527850 | -0.2685900 |
| C | 4.6264460 | 1.3208410 | -0.1558440 |
| S | 0.0548190 | 1.0183810 | -0.1419190 |
| C | -1.1860880 | -0.2379570 | -0.0121760 |
| C | -2.5197200 | 0.1174700 | -0.0780470 |
| C | -3.5590220 | -0.8303540 | -0.0034180 |

| | | | |
|---|------------|------------|------------|
| C | -3.1719140 | -2.2029260 | 0.0275380 |
| C | -1.8146990 | -2.5469590 | 0.1290490 |
| C | -0.8219750 | -1.5908990 | 0.1360270 |
| C | -4.1536640 | -3.2199710 | -0.1331020 |
| C | -5.4431580 | -2.8932370 | -0.3852130 |
| C | -5.8736740 | -1.5348210 | -0.3677540 |
| C | -4.9687740 | -0.4999420 | -0.0587740 |
| C | -7.2335320 | -1.2405460 | -0.6689880 |
| C | -7.7005530 | 0.0303570 | -0.6373170 |
| C | -6.8687810 | 1.0853920 | -0.1714710 |
| C | -5.5156300 | 0.8186050 | 0.1849380 |
| C | -7.4047510 | 2.3767550 | 0.0089850 |
| C | -6.6707170 | 3.3757250 | 0.5938130 |
| C | -5.3779870 | 3.0915920 | 1.0560420 |
| C | -4.8211520 | 1.8512380 | 0.8579760 |
| S | 0.8758290 | -2.0687200 | 0.2654210 |
| H | -2.7501520 | 1.1621500 | -0.2517350 |
| H | -3.8445730 | 1.6534820 | 1.2801560 |
| H | -4.8155840 | 3.8501890 | 1.5915610 |
| H | -7.0979900 | 4.3632460 | 0.7356770 |
| H | -8.4315850 | 2.5541100 | -0.3010580 |
| H | -8.7281140 | 0.2578660 | -0.9078790 |
| H | -7.8840560 | -2.0647310 | -0.9500950 |
| H | -6.1845000 | -3.6628480 | -0.5830820 |
| H | -3.8340270 | -4.2584990 | -0.1074630 |
| H | -1.5479870 | -3.6015440 | 0.1683740 |
| H | 1.7956250 | 2.9741850 | -0.4012520 |
| H | 3.3447440 | 4.8936100 | -0.6124740 |
| H | 5.8149220 | 4.4643820 | -0.5216600 |
| H | 6.6097950 | 2.1442630 | -0.2272200 |
| H | 7.1343310 | 0.1815290 | 0.0096950 |
| H | 7.6034280 | -2.2257790 | 0.3042620 |
| H | 5.6752880 | -3.8213110 | 0.4738000 |
| H | 3.3719890 | -2.9219860 | 0.3408080 |

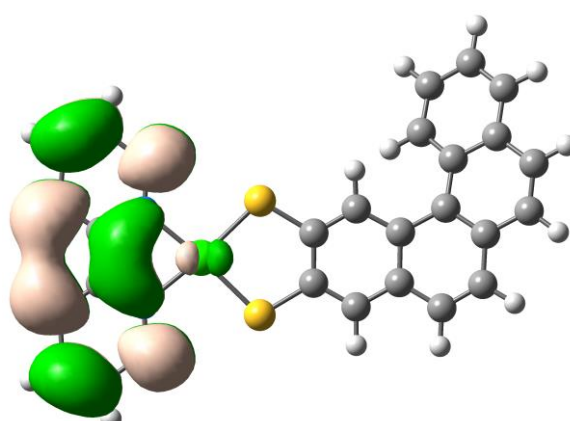
Mulliken charges with hydrogens summed into heavy atoms (in electrons)

| | |
|------|-----------|
| 1 C | 0.341101 |
| 2 N | -0.693781 |
| 3 C | 0.281752 |
| 4 C | 0.050747 |
| 5 C | 0.153605 |
| 6 C | -0.026953 |
| 7 Pt | 0.490830 |
| 8 N | -0.694477 |
| 9 C | 0.341511 |
| 10 C | -0.026735 |
| 11 C | 0.153733 |
| 12 C | 0.050755 |
| 13 C | 0.282082 |

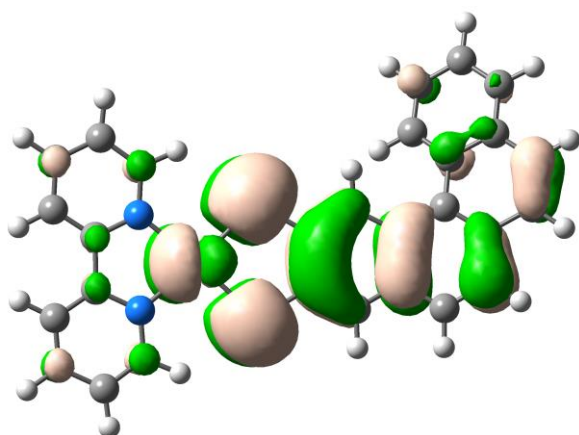
| | | |
|----|---|-----------|
| 14 | S | -0.149149 |
| 15 | C | -0.189943 |
| 16 | C | 0.066642 |
| 17 | C | -0.044706 |
| 18 | C | -0.080432 |
| 19 | C | 0.041525 |
| 20 | C | -0.176668 |
| 21 | C | 0.037998 |
| 22 | C | 0.018511 |
| 23 | C | -0.067295 |
| 24 | C | -0.030755 |
| 25 | C | 0.023777 |
| 26 | C | 0.044709 |
| 27 | C | -0.084065 |
| 28 | C | -0.039329 |
| 29 | C | 0.026206 |
| 30 | C | 0.006695 |
| 31 | C | -0.004299 |
| 32 | C | 0.042612 |
| 33 | S | -0.146205 |



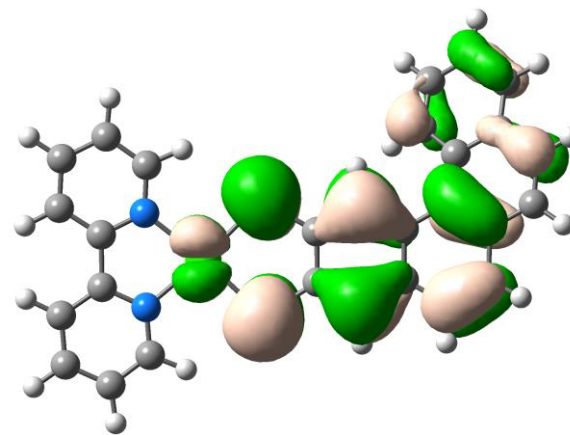
LUMO (-2.58 eV)



LUMO+1 (-1.67 eV)



HOMO (-5.51 eV)



HOMO-1 (-5.58 eV)

Fig. S13 Frontier orbitals plots with an isovalue of 0.02 au.

Table S7. Excited singlet states calculated energies (eV), oscillator and rotatory strengths (cgs), as well as main MO composition for the 5 lowest singlet states with an oscillator strength larger than 0.02.

| Excited-state | ΔE | f | $Rot.$ | Composition |
|-----------------------|------------|------|--------|---------------|
| S₁ | 2.23 | 0.21 | -8.39 | HOMO-LUMO |
| S₆ | 3.11 | 0.12 | -29.4 | HOMO-LUMO+2 |
| S₈ | 3.17 | 0.03 | 19.5 | HOMO-1-LUMO+1 |
| S₁₂ | 3.46 | 0.35 | -39.9 | HOMO-1-LUMO+4 |
| S₁₃ | 3.53 | 0.23 | -35.0 | HOMO-3-LUMO |

The density difference plot corresponding to the lowest excited singlet state is showed below in Figure S14. As can be seen, there is a significant CT involved in this transition, the electron going from the helicene side to the bi-pyridyl moiety. Using Le Bahers' metric, we determine a significant CT distance and dipole moment of 4.04 Å and 18.1 D, respectively. As these values are rather large, this might suggest that the M06 functional is not the most suited to model this transition. For this reason, we have performed the same calculation with M06-2X that encompasses a double amount of *exact* exchange. As can be seen in Figure S14, we obtained qualitatively the same results in terms of density reorganization, and this holds for the CT parameters that attain 3.80 Å for the distance and 18.5 D for the dipole, both values being very close to their M06 counterpart.

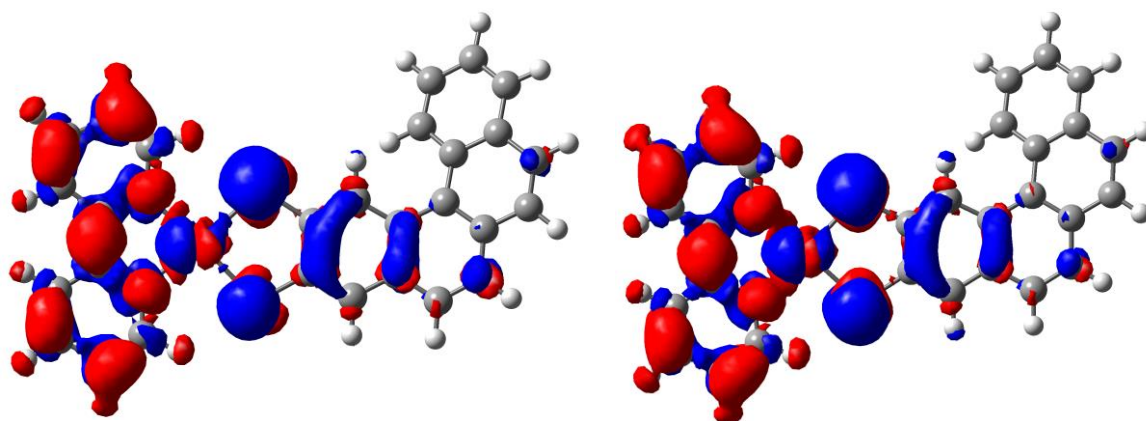


Fig. S14 Difference density representation between the first excited-state and the ground state obtained at the M06 (left) and M06-2X (right) levels of theory. The blue and red regions indicate loss and gain of electron density, respectively. Isovalue: 1×10^{-3} a.u.

Excited states relaxation and emission

Below are given the total M06 energy and Cartesian coordinates of the lowest triplet state, as obtained by a U-DFT optimization.

Total electronic energy -2102.29163880au

Cartesian coordinates (in Å)

| | | | |
|----|------------|------------|------------|
| C | 4.2131750 | -2.2648180 | 0.2989130 |
| N | 3.9394300 | -0.9561930 | 0.1264070 |
| C | 4.9831080 | -0.0475740 | 0.0084800 |
| C | 6.3108140 | -0.5239260 | 0.0747280 |
| C | 6.5653910 | -1.8543910 | 0.2509190 |
| C | 5.4868130 | -2.7608620 | 0.3671470 |
| Pt | 2.0696430 | -0.1036640 | 0.0132230 |
| N | 3.2528810 | 1.5696530 | -0.2134220 |
| C | 2.8259670 | 2.8364450 | -0.3802290 |
| C | 3.6750000 | 3.9023750 | -0.5137990 |
| C | 5.0661190 | 3.6585360 | -0.4739710 |
| C | 5.5209070 | 2.3813640 | -0.3057770 |
| C | 4.6147800 | 1.3064900 | -0.1715110 |
| S | 0.0380680 | 0.9926610 | -0.1404250 |
| C | -1.1654830 | -0.2422890 | -0.0230070 |
| C | -2.5133830 | 0.1142930 | -0.0926560 |
| C | -3.5350830 | -0.8281130 | -0.0093250 |
| C | -3.1435300 | -2.2142030 | 0.0168840 |
| C | -1.8005570 | -2.5657350 | 0.1261180 |
| C | -0.7961730 | -1.6082420 | 0.1351970 |
| C | -4.1303600 | -3.2268990 | -0.1622120 |
| C | -5.4103940 | -2.8879560 | -0.4284300 |
| C | -5.8449970 | -1.5241800 | -0.3998470 |
| C | -4.9489740 | -0.4958070 | -0.0635200 |
| C | -7.2005910 | -1.2323460 | -0.7026970 |
| C | -7.6693890 | 0.0400940 | -0.6482180 |
| C | -6.8438420 | 1.0865150 | -0.1624130 |
| C | -5.4906900 | 0.8165530 | 0.1963210 |
| C | -7.3814110 | 2.3763740 | 0.0317410 |
| C | -6.6481390 | 3.3664550 | 0.6292120 |
| C | -5.3548140 | 3.0774900 | 1.0912710 |
| C | -4.7957120 | 1.8415720 | 0.8816850 |
| S | 0.8667950 | -2.0772080 | 0.2801710 |
| H | -2.7423890 | 1.1585660 | -0.2661970 |
| H | -3.8203480 | 1.6407470 | 1.3054790 |
| H | -4.7953010 | 3.8308050 | 1.6367310 |
| H | -7.0748330 | 4.3522840 | 0.7823980 |
| H | -8.4070380 | 2.5572190 | -0.2790980 |
| H | -8.6957140 | 0.2699040 | -0.9204920 |
| H | -7.8488020 | -2.0515590 | -1.0010260 |
| H | -6.1526520 | -3.6524750 | -0.6405920 |
| H | -3.8167060 | -4.2663140 | -0.1404830 |
| H | -1.5355620 | -3.6194910 | 0.1628630 |

| | | | |
|---|-----------|------------|------------|
| H | 1.7501960 | 2.9813740 | -0.4051240 |
| H | 3.2732770 | 4.8990530 | -0.6454540 |
| H | 5.7695980 | 4.4780320 | -0.5754450 |
| H | 6.5864330 | 2.1835800 | -0.2730120 |
| H | 7.1312850 | 0.1790320 | -0.0161240 |
| H | 7.5887340 | -2.2108370 | 0.3007040 |
| H | 5.6459790 | -3.8225250 | 0.5069970 |
| H | 3.3563480 | -2.9263360 | 0.3835910 |

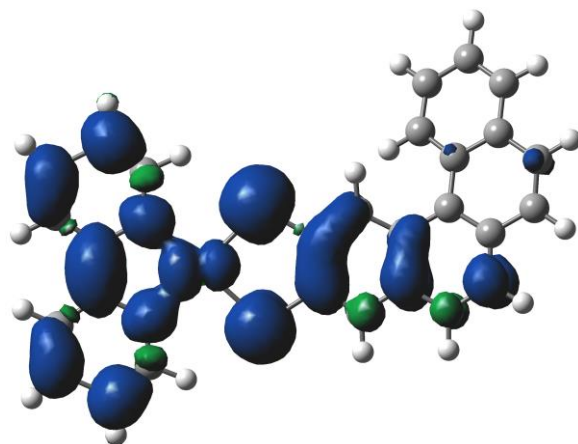
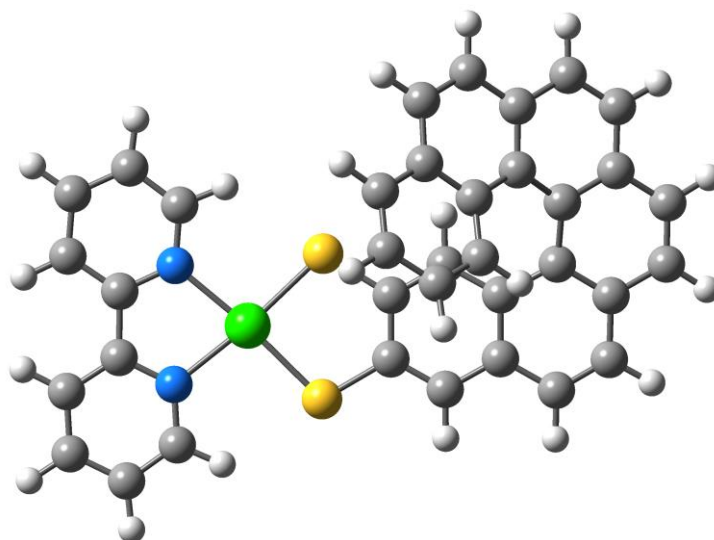


Fig. S15 Density difference plots for the T₁ state. Isovalue: 1 x 10⁻³ a.u.

(P)-2b**Fig. S16** DFT-optimized equilibrium geometry for *(P)*-2b.**Equilibrium ground-state geometry and energy [M06 level]**

Total electronic energy -2409.46343392au

Cartesian coordinates (in Å)

| | | | |
|----|------------|------------|------------|
| Pt | -2.4960400 | -0.3105540 | -0.2514370 |
| S | -0.4276810 | 0.5884710 | -0.7527020 |
| S | -1.4403120 | -2.3185830 | 0.1938270 |
| N | -3.6001540 | 1.4293610 | -0.5852070 |
| N | -4.4413710 | -0.9593870 | 0.1443280 |
| C | 0.7257210 | -0.7195950 | -0.4510620 |
| C | 2.0747170 | -0.4731740 | -0.5968170 |
| H | 2.3811610 | 0.5171340 | -0.9200690 |
| C | 3.0449830 | -1.4497020 | -0.3249860 |
| C | 4.4681520 | -1.1890290 | -0.3652930 |
| C | 5.0534780 | 0.1296380 | -0.3654540 |
| C | 4.4452650 | 1.3194500 | 0.1833360 |
| C | 3.4833970 | 1.3252930 | 1.2669520 |
| C | 3.2773030 | 0.2247020 | 2.1254070 |
| H | 3.8888900 | -0.6631490 | 2.0082590 |
| C | 2.3277340 | 0.2532360 | 3.1166720 |
| H | 2.1996400 | -0.6097360 | 3.7629670 |
| C | 1.5313840 | 1.3934850 | 3.3056420 |
| H | 0.7677690 | 1.4034730 | 4.0769350 |
| C | 1.7574990 | 2.5068920 | 2.5374680 |
| H | 1.1904810 | 3.4192950 | 2.7046130 |
| C | 2.7511750 | 2.5103230 | 1.5370850 |
| C | 3.0723050 | 3.7125450 | 0.8423310 |
| H | 2.4918950 | 4.6067840 | 1.0528140 |

| | | | |
|---|------------|------------|------------|
| C | 4.1373100 | 3.7517920 | 0.0071610 |
| H | 4.4516160 | 4.6852820 | -0.4523030 |
| C | 4.8718080 | 2.5702510 | -0.3082390 |
| C | 6.0522930 | 2.6636930 | -1.0907880 |
| H | 6.3695120 | 3.6434680 | -1.4372360 |
| C | 6.8100440 | 1.5599980 | -1.3179230 |
| H | 7.7722740 | 1.6337350 | -1.8174390 |
| C | 6.3336780 | 0.2720500 | -0.9590290 |
| C | 7.1346310 | -0.8736570 | -1.2005060 |
| H | 8.1306460 | -0.7310060 | -1.6108250 |
| C | 6.6792130 | -2.1128620 | -0.8789710 |
| H | 7.3145720 | -2.9878950 | -0.9867860 |
| C | 5.3293060 | -2.3001030 | -0.4859820 |
| C | 4.8339510 | -3.6174180 | -0.2472830 |
| H | 5.5401590 | -4.4427980 | -0.2835790 |
| C | 3.5266670 | -3.8335840 | 0.0351660 |
| H | 3.1610670 | -4.8328840 | 0.2571520 |
| C | 2.5875630 | -2.7636280 | -0.0332320 |
| C | 1.2119110 | -3.0009540 | 0.1213920 |
| H | 0.8797320 | -4.0083870 | 0.3655410 |
| C | 0.2821180 | -1.9952950 | -0.0477850 |
| C | -3.0917250 | 2.6126720 | -0.9516870 |
| H | -2.0157340 | 2.6564400 | -1.0841040 |
| C | -3.8815270 | 3.7262880 | -1.1534270 |
| H | -3.4215050 | 4.6606160 | -1.4500980 |
| C | -5.2509990 | 3.6164360 | -0.9689900 |
| H | -5.9009340 | 4.4708650 | -1.1179640 |
| C | -5.7807330 | 2.3969280 | -0.5901010 |
| H | -6.8477530 | 2.2919710 | -0.4398270 |
| C | -4.9368050 | 1.3105210 | -0.4029390 |
| C | -5.4051190 | -0.0193710 | -0.0017500 |
| C | -6.7403440 | -0.3277640 | 0.2210430 |
| H | -7.5041810 | 0.4297460 | 0.0991960 |
| C | -7.0915950 | -1.6106190 | 0.5983010 |
| H | -8.1311340 | -1.8621220 | 0.7738800 |
| C | -6.0964580 | -2.5641260 | 0.7468240 |
| H | -6.3236600 | -3.5811810 | 1.0411050 |
| C | -4.7862360 | -2.2001360 | 0.5111430 |
| H | -3.9772050 | -2.9155180 | 0.6159600 |

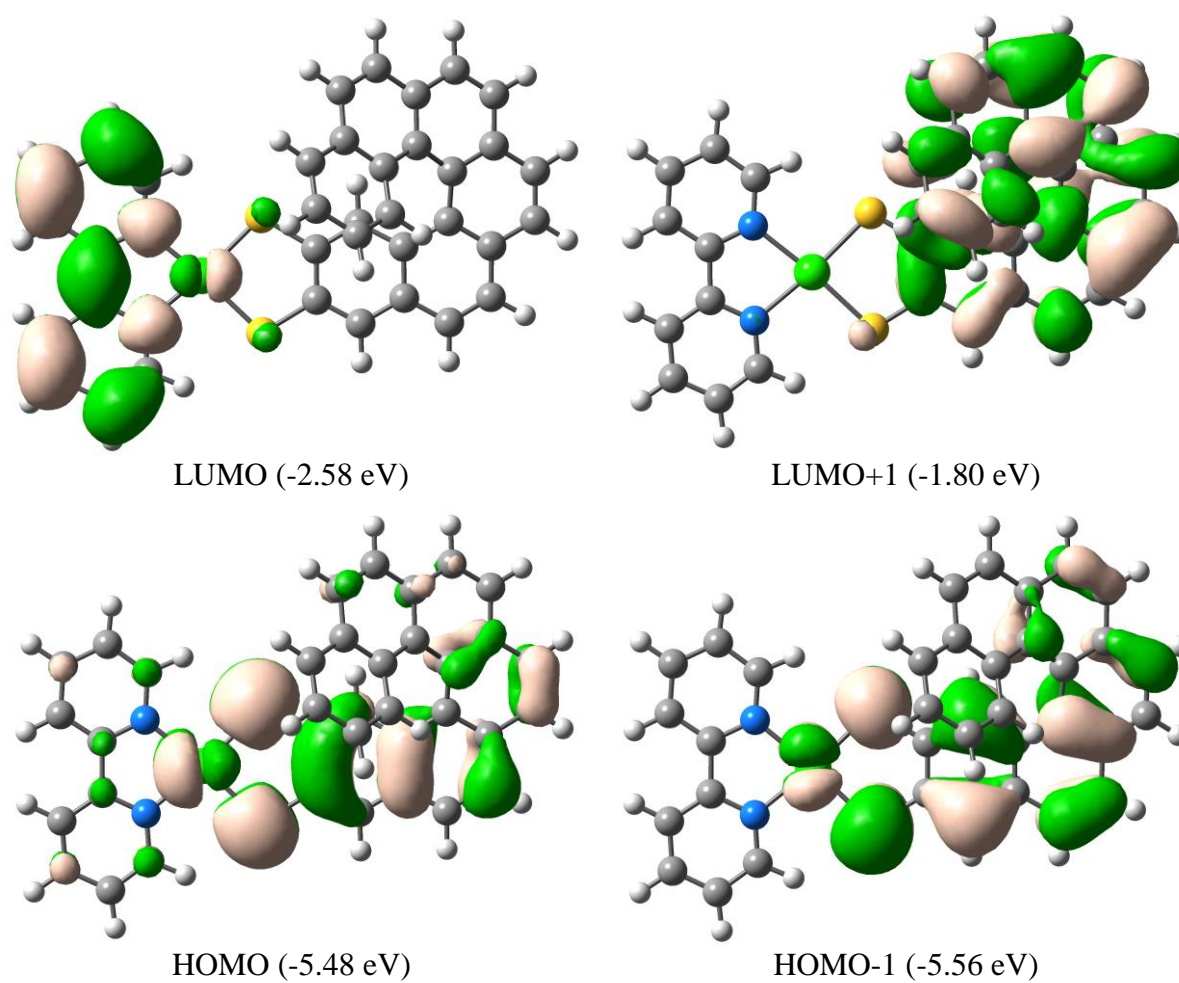


Fig. S17 Frontier orbitals plots with an isovalue of 0.02 au.

Table S8. Singlet excited-state energies (eV), oscillator and rotatory strengths (cgs), as well as main MO composition for the 5 lowest singlet states with an oscillator strength larger than 0.02.

| Excited-state | ΔE | f | $Rot.$ | Composition |
|-----------------------|------------|------|--------|---------------|
| S₁ | 2.21 | 0.19 | 17.32 | HOMO-LUMO |
| S₄ | 2.93 | 0.04 | 73.1 | HOMO-LUMO+1 |
| S₈ | 3.14 | 0.26 | 339.5 | HOMO-1-LUMO+3 |
| S₁₁ | 3.18 | 0.02 | -8.6 | HOMO-LUMO+3 |
| S₁₅ | 3.47 | 0.04 | 13.0 | HOMO-1-LUMO+4 |

| | | | |
|---|------------|------------|------------|
| H | 0.5648780 | 1.4003150 | 3.9409490 |
| C | 1.6303380 | 2.5141230 | 2.4610210 |
| H | 1.0575230 | 3.4262720 | 2.6072350 |
| C | 2.6681800 | 2.5213420 | 1.5062160 |
| C | 3.0166910 | 3.7246860 | 0.8289490 |
| H | 2.4302560 | 4.6190350 | 1.0207840 |
| C | 4.1085150 | 3.7643240 | 0.0287020 |
| H | 4.4387120 | 4.6979830 | -0.4185140 |
| C | 4.8487470 | 2.5823850 | -0.2665350 |
| C | 6.0502940 | 2.6792960 | -1.0186040 |
| H | 6.3740140 | 3.6608110 | -1.3533120 |
| C | 6.8156260 | 1.5798720 | -1.2306790 |
| H | 7.7890940 | 1.6563460 | -1.7066670 |
| C | 6.3325240 | 0.2895450 | -0.8862650 |
| C | 7.1373510 | -0.8496500 | -1.1225050 |
| H | 8.1402370 | -0.7020720 | -1.5131410 |
| C | 6.6774130 | -2.0966550 | -0.8271000 |
| H | 7.3156210 | -2.9691060 | -0.9333620 |
| C | 5.3243160 | -2.2834770 | -0.4633850 |
| C | 4.8271130 | -3.6082900 | -0.2360840 |
| H | 5.5403540 | -4.4275350 | -0.2663860 |
| C | 3.5240380 | -3.8401200 | 0.0404430 |
| H | 3.1662500 | -4.8418750 | 0.2591320 |
| C | 2.5765320 | -2.7759680 | -0.0296190 |
| C | 1.2132420 | -3.0256030 | 0.1194130 |
| H | 0.8856600 | -4.0334030 | 0.3624280 |
| C | 0.2693290 | -2.0234550 | -0.0608970 |
| C | -3.0255430 | 2.6131160 | -0.9627690 |
| H | -1.9503620 | 2.6489720 | -1.1101960 |
| C | -3.7914550 | 3.7317400 | -1.1558360 |
| H | -3.3238980 | 4.6604910 | -1.4573750 |
| C | -5.1858270 | 3.6311000 | -0.9514560 |
| H | -5.8250020 | 4.4956910 | -1.0953340 |
| C | -5.7254850 | 2.4349850 | -0.5715410 |
| H | -6.7944230 | 2.3464670 | -0.4129230 |
| C | -4.9033940 | 1.3024260 | -0.3814870 |
| C | -5.3626230 | 0.0227250 | 0.0089220 |
| C | -6.7101360 | -0.3099220 | 0.2698280 |
| H | -7.4731140 | 0.4542820 | 0.1719370 |
| C | -7.0547510 | -1.5781840 | 0.6420310 |
| H | -8.0924960 | -1.8243150 | 0.8403360 |
| C | -6.0500930 | -2.5649480 | 0.7671940 |
| H | -6.2813760 | -3.5812240 | 1.0600810 |
| C | -4.7547900 | -2.2074900 | 0.5074990 |
| H | -3.9524940 | -2.9342140 | 0.5928320 |

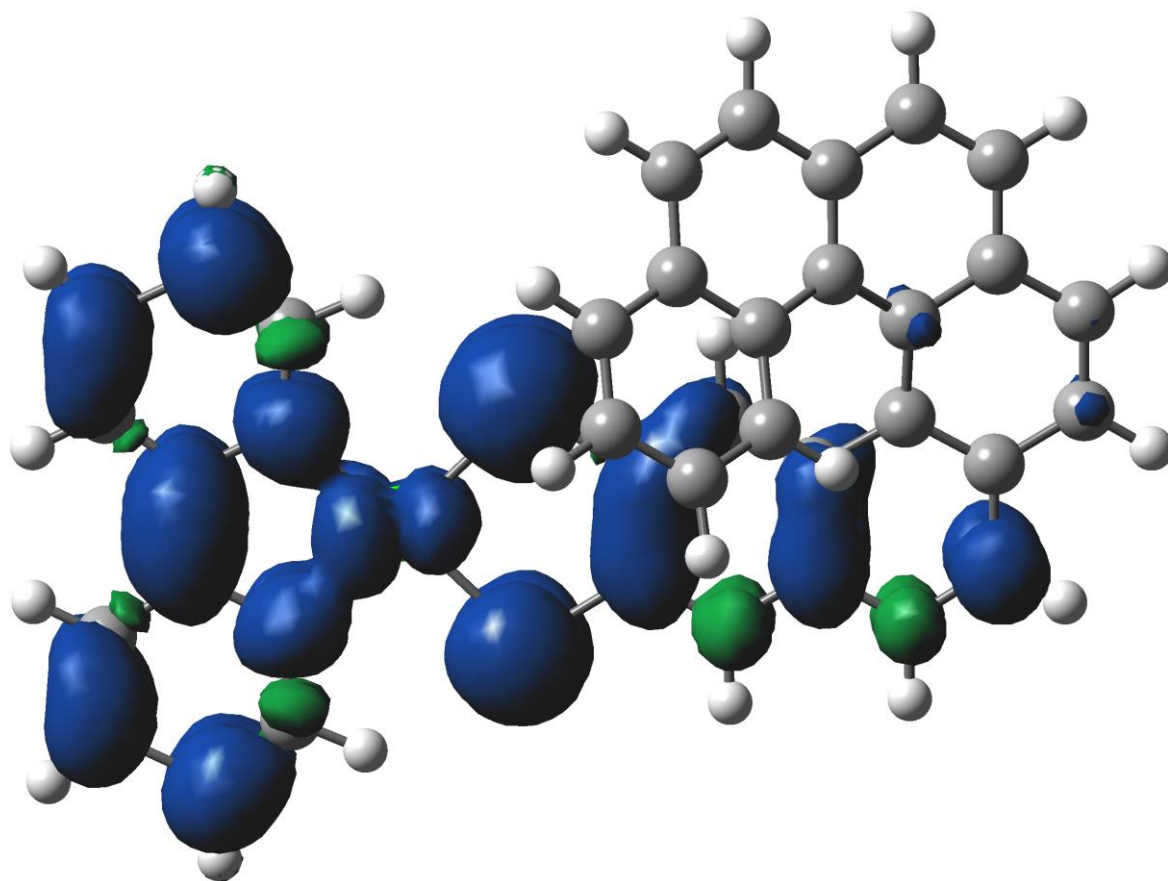


Fig. S19 Density difference plots for the T₁ state. Isovalue: 1×10^{-3} a.u.

CD spectroscopy

CD spectra for (*P*)- and (*M*)-**2b** were recorded at concentrations of 2.4×10^{-4} M in acetonitrile in 1 cm quartz suprasil cuvettes on a JASCO J-815 CD spectrometer.

CPL measurement, modified ROA instrument

The CPL of compounds (*P*) and (*M*)-**2b** were measured with a spectrometer conceived for Raman optical activity measurements.^[1] The wavelength of the exciting radiation is 532 nm (SHG Nd:YAG). In order to meet the spectral range requirements for the luminescence of **2b**, the broadband HFG-730.8 holographic grating from Kaiser Optical Systems, Inc. (KOSI) was utilized. It showed a spectral coverage from 557.3 to 904.3 nm, and a linear dispersion of 0.35 nm/pixel. The spectrograph was equipped with a cooled, low noise, back-illuminated CCD camera from Critical Link (MityCCD-E3011-BI, 1024 × 256 pixels of 26 μm × 26 μm). All polarization optics in the light collection train of the spectrometer was exchanged to account for the larger spectral range of operation. The clear aperture diameter of the light collection was reduced from 28 to 23 mm due to smaller optics used. The liquid crystal retarder voltage was optimized for the center of the spectral window.

References

- [1] Werner, H.; Hangartner, G. *J. Raman Spectrosc.*, **1999**, *30*, 841–852.
- [2] Longhi, G.; Castiglioni, E.; Abbate, S.; Lebon, F.; Lightner, D. A. *Chirality* **2013**, *25*, 589–599.
- [3] Pecul, M.; Ruud, K. *Phys Chem Chem Phys* **2011**, *13*, 643–650.
- [4] Pritchard, B.; Autschbach, J. *ChemPhysChem* **2010**, *11*, 2409–2415.
- [5] Zhao, Y.; Truhlar, D. G. *Theor. Chem. Acc.* **2008**, *120*, 215–241.
- [6] Perdew, J. P.; Burke, K.; Ernzerhof, M. *Phys. Rev. Lett.* **1996**, *77*, 3865–3868.
- [7] Adamo, C.; Barone, V. *J. Chem. Phys.* **1999**, *110*, 6158–6170.
- [8] Biet, T.; Fihey, A.; Cauchy, T.; Vanthuyne, N.; Roussel, C.; Crassous, J.; Avarvari, N. *Chem. - Eur. J.* **2013**, *19*, 13160–13167.
- [9] Frisch, M. J.; Trucks, G. W.; Schlegel, H. B.; Scuseria, G. E.; Robb, M. A.; Cheeseman, J. R.; Scalmani, G.; Barone, V.; Mennucci, B.; Petersson, G. A.; Nakatsuji, H.; Caricato, M.; Li, X.; Hratchian, H. P.; Izmaylov, A. F.; Bloino, J.; Zheng, G.; Sonnenberg, J. L.; Hada, M.; Ehara, M.; Toyota, K.; Fukuda, R.; Hasegawa, J.; Ishida, M.; Nakajima, T.; Honda, Y.; Kitao, O.; Nakai, H.; Vreven, T.; Montgomery, J. A., Jr.; Peralta, J. E.; Ogliaro, F.; Bearpark, M.; Heyd, J. J.; Brothers, E.; Kudin, K. N.; Staroverov, V. N.; Kobayashi, R.; Normand, J.; Raghavachari, K.; Rendell, A.; Burant, J. C.; Iyengar, S. S.; Tomasi, J.; Cossi, M.; Rega, N.; Millam, J. M.; Klene, M.; Knox, J. E.; Cross, J. B.; Bakken, V.; Adamo, C.; Jaramillo, J.; Gomperts, R.; Stratmann, R. E.; Yazyev, O.; Austin, A. J.; Cammi, R.; Pomelli, C.; Ochterski, J. W.; Martin, R. L.; Morokuma, K.; Zakrzewski, V. G.; Voth, G. A.; Salvador, P.; Dannenberg, J. J.; Dapprich, S.; Daniels, A. D.; Farkas, Ö.; Foresman, J. B.; Ortiz, J. V.; Cioslowski, J.; Fox, D. J. *Gaussian 09 Revision D.01*.
- [10] Morille, Y.; Cauchy, T. *ABSiCC Automating Boring Stuff in Computational Chemistry*; University of Angers, 2014.
- [11] O'boyle, N. M.; Tenderholt, A. L.; Langner, K. M. *J. Comput. Chem.* **2008**, *29*, 839–845.
- [12] Le Bahers, T.; Adamo, C.; Ciofini, I. *J. Chem. Theory Comput.* **2011**, *8*, 2498–2506.